Letter

Leaky exciton condensates in transition metal dichalcogenide moiré bilayers

Benjamin Remez [1,*] and Nigel R. Cooper [1,2]

[1] *T.C.M. Group, Cavendish Laboratory, University of Cambridge, JJ Thomson Avenue, Cambridge CB3 0HE, United Kingdom*

[2] *Department of Physics and Astronomy, University of Florence, Via G. Sansone 1, 50019 Sesto Fiorentino, Italy*

(Received 20 October 2021; revised 18 March 2022; accepted 22 March 2022; published 24 May 2022)

We show that the "dark condensates" that arise when excitons form a Bose-Einstein condensate in a material with an indirect band gap are not completely dark to optical emission. Rather, such states are "leaky condensates" in which optical emission is facilitated by many-body interactions. We analyze the properties of these leaky condensates in the context of twisted bilayers of transition metal dichalcogenides, which host strongly interacting excitons and an indirect band gap. We show that this interaction-driven "leaky" emission dominates photoluminescence at low temperatures, with distinctive qualitative features. Finally, we propose that in these materials unique intervalley physics can lead to crystal symmetry-breaking excitonic ordering, with implications for optical processes.

DOI: 10.1103/PhysRevResearch.4.L022042

Excitons, bound electron-hole (e-h) pairs, give rise to a plethora of quantum-coherent phenomena in solids, including light-matter hybridization [1,2], long-range order [3], phase coherence [4], and Bose-Einstein condensates (BECs) [5]. Novel atomically thin transition metal dichalcogenide (TMD) structures [6], featuring tightly-bound excitons with long lifetime [7–12] and valley pseudospin with contrasting optical selection rules [13], have spearheaded a new generation of excitonic devices. In parallel, the maturing field of twistronics [14] predicts phenomena such as flat [15] and topological excitonic bands with chiral edge modes [16]. This versatility is promising for realizing quantum emitters [17,18], simulators [19], and exciton BECs [20,21], and many-body exciton physics is being explored in electrostatically gated, optically inert excitonic insulators [22–28] and cavity exciton-polaritons [29–33].

In twisted TMD heterobilayers, interlayer excitons [34] formed by electrons and holes in opposite layers lie at low energies [35], and provide a compelling platform for pumped exciton condensates. First, the spatial separation of electrons and holes leads to long exciton lifetimes. The interlayer twist then rotates electron bands in momentum space [36], resulting in an indirect band gap [37] and even longer lifetimes [7,38]. Second, the misaligned layers form a large-scale moiré superlattice, with a spatially modulated band gap [17,39–43] that traps excitons in localized orbitals [44–48]. This, and the excitons' interlayer electric dipole, place them in the strongly interacting regime [17]. These BECs thus merge strong correlations, quasiequilibrium dynamics, and opto-, twist-, and valleytronics. Clearly, new approaches are called for.

In this Letter we show that the intersection of strong interactions and indirect gap leads to striking optical properties in these moiré BECs. The indirect band gap suggests that the exciton ground state forms a so-called dark condensate that cannot emit light directly [49]. However, as we will show, no condensate is completely dark if interactions are considered. In this strongly interacting system such effects are dominant, driving emission from the BEC even at vanishing temperature, which we describe as a "leaky condensate." These "leaks" give rise to distinctive qualitative features in the optical emission of TMD moiré excitons at low temperatures.

Model. We consider a tight-binding lattice model for the interlayer excitons on the TMD moiré superlattice, as proposed in previous works [17,40,47–49]. The superlattice inherits the triangular symmetry of the underlying monolayers, and has three high-symmetry locations labeled A, B, and C, as seen in Fig. 1(a) [50]. Sites A and B are local energy minima hosting bound states while C is a higher local energy maximum. A and B are generally not degenerate, and their energetic ordering may depend on the choice of monolayer compounds and whether they are stacked near 0 or 180 degrees [17,40]. However, for simplicity we consider only the lowest-energy locale and our results hold whether it is A or B. Additionally, the triangular symmetry of each monolayer lends it a hexagonal Brillouin zone, with gapped valleys at the two inequivalent $\pm K$-point corners. e-h pairs are pumped optically via vertical interband transitions, and so excitons can be photogenerated in either valley, labeled by $\tau = \pm 1$ [13].

We thus consider the Bose-Hubbard [51] Hamiltonian

$$\hat{H} = \sum_{\mathbf{k},\tau} (E_0 + \epsilon_{\mathbf{k}}) \hat{\chi}^{\dagger}_{\mathbf{k}\tau} \hat{\chi}_{\mathbf{k}\tau} + \sum_{\mathbf{R},\tau,\sigma} \frac{U_{\tau\sigma}}{2} \hat{\chi}^{\dagger}_{\mathbf{R}\tau} \hat{\chi}^{\dagger}_{\mathbf{R}\sigma} \hat{\chi}_{\mathbf{R}\sigma} \hat{\chi}_{\mathbf{R}\tau} + \hat{V}_{\mathrm{LMI}}, \tag{1}$$

*br395@cam.ac.uk

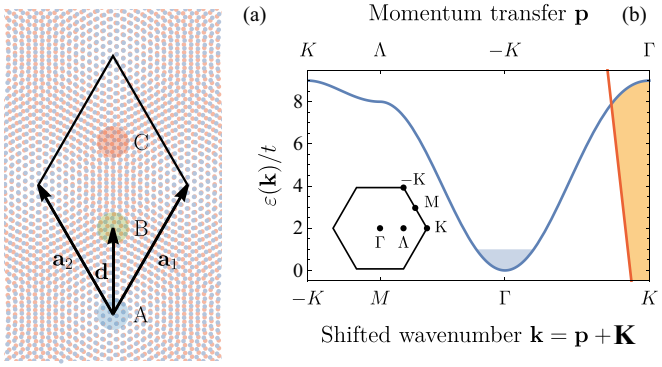

FIG. 1. (a) The moiré triangular superlattice formed by a twist of 3°. The diamond outlines the moiré unit cell, with the three high-symmetry rotation centers A, B, and C highlighted in blue, green, and red. (b) 5. The nearest-neighbor-hopping exciton dispersion in the moiré Brillouin zone. The blue and orange regions represent the condensate and the optical light cone (of $\tau = +1$ excitons, not to scale) respectively.

where $\hat{\chi}^\dagger_{\mathbf{R}\tau}$ is the bosonic creation operator of the lowest Wannier state in supercell $\mathbf{R}$ (at either locale A or B) and valley τ. $\hat{\chi}^\dagger_{\mathbf{k}\tau}$, defined shortly, creates plane-wave states with dispersion $\epsilon_{\mathbf{k}}$. We use $\epsilon_{\mathbf{k}} = -t[4\cos(k_x a/2)\cos(\sqrt{3}k_y a/2) + 2\cos(k_x a) - 6]$, corresponding to nearest-neighbor hopping with amplitude $t > 0$ and moiré period a [50], and plotted in Fig. 1(b). E_0 is the exciton formation energy (band gap minus binding energy). $U_{\tau\sigma} > 0$ are valley-dependent [52] on-site repulsion strengths; due to moiré localization a strongly interacting system with $t/U_{\tau\sigma} < 0.1$ is predicted [17,49], which we will treat accordingly. $\hat{V}_{\mathrm{LMI}}$ is the light-matter interaction, addressed below.

A specific gauge is fixed in Eq. (1): Exciton momentum eigenstates superpose e-h pairs with fixed momentum transfer $\mathbf{p}_e - \mathbf{p}_h = \mathbf{p}$. Due to the indirect gap, the lowest-energy transition occurs at $\mathbf{p} = -\tau\mathbf{K} \neq \mathbf{0}$, where $\mathbf{K} = \mathbf{K}_h - \mathbf{K}_e$ is the momentum mismatch between the $\tau = +1$ valley extrema of the two layers [17,36,37], coinciding with the moiré Brillouin zone (MBZ) corner. It is convenient to define the shifted wave vector $\mathbf{k} = \mathbf{p} + \tau\mathbf{K}$, so real- and $\mathbf{k}$-space states are related by

$$\hat{\chi}_{\mathbf{k}\tau} = \frac{1}{\sqrt{N}} \sum_{\mathbf{R}} e^{-i(\mathbf{k}-\tau\mathbf{K})\cdot\mathbf{R}} \hat{\chi}_{\mathbf{R}\tau} \tag{2}$$

with N the number of supercells. Indeed, the hopping amplitudes $\langle \mathbf{R}\tau|\hat{H}|\mathbf{R}'\tau\rangle$ are complex. Their phases are fixed by the momentum mismatch [17], which guarantees [50] that in this unique gauge $\epsilon_{\mathbf{k}}$ is valley independent and minimal at $\mathbf{k} = \mathbf{0}$.

This momentum mismatch implies that the excitonic ground states cannot recombine radiatively: The nearly vertical photon dispersion gives rise to the well-known optical light cone (LC) of states with $|\mathbf{p}| \lesssim E_0/\hbar c$ that can recombine, with c the speed of light in the surrounding medium. The light cone of each valley is thereby centered at $\mathbf{k} = \tau\mathbf{K}$, i.e., the MBZ corners; see Fig. 1(b). Crucially, the $\mathbf{k} = \mathbf{0}$ states lie outside both cones, and thus they are momentum dark.

Under a broad set of conditions, the Hamiltonian (1) has a many-body ground state that is Bose-condensed, with a large phase-coherent occupation of the single-particle ground states at $\mathbf{k} = \mathbf{0}$. In direct-gap systems, where these states are bright, this would lead to a pronounced phase-coherent emission similar to superradiance [5]. Yet the twist-induced momentum mismatch renders the BEC a "dark condensate" from which direct optical emission is forbidden by translation symmetry.

Breaking translation symmetry can enable emission from momentum-dark excitons. This has been realized externally in TMDs, with electronic charge order [53,54] and incommensurate substrates [55]. Indeed, translation symmetry breaking is a hallmark of indirect-gap exciton coherence [22,56,57]. The interplay of two interacting valleys in Hamiltonian (1) can cause the excitons to break translation symmetry and form exciton density waves, which we explore in the Supplemental Material [50]. We find that while these density waves have precisely the required geometry, threefold rotation symmetry prevents direct emission and the condensate remains dark.

Leaky condensates. While its coherent component cannot emit directly, the many-body condensed ground state is not completely dark. Rather, exciton-exciton interactions induce an incoherent component that can radiate. Emission is driven by excitonic collective modes [58], which have attracted recent attention as insightful probes of excitonic many-body states [57,59–64]. Here, the collective modes supply the momentum necessary for the excitons to recombine. Collective modes exist in normal phases, and so Bose coherence is not a prerequisite for this mechanism. However, below we demonstrate that in twisted bilayers this is the dominant emission channel at low temperatures. Thus, many-body interaction effects will determine the optical character of the low-temperature condensed phases, which we call "leaky condensates."

The essential physics of our mechanism is captured by a single-valley model. This may be realized experimentally by pumping a valley-contrasting circularly polarized intralayer exciton resonance, followed by rapid interlayer charge transfer [65]. Excitons exhibit long valley depolarization times [11,48,65,66] thanks to the large e-h vertical separation [34], suggesting the exciton population can be treated as valley polarized over radiative timescales. Projecting onto valley $\tau = +1$ and suppressing τ henceforth, $\hat{H}$ reduces to

$$\hat{H} = \sum_{\mathbf{k}} (E_0 + \epsilon_{\mathbf{k}}) \hat{\chi}^\dagger_{\mathbf{k}} \hat{\chi}_{\mathbf{k}} + \frac{U}{2} \sum_{\mathbf{R}} \hat{\chi}^\dagger_{\mathbf{R}} \hat{\chi}^\dagger_{\mathbf{R}} \hat{\chi}_{\mathbf{R}} \hat{\chi}_{\mathbf{R}} + \hat{V}_{\mathrm{LMI}}. \tag{3}$$

Equation (2) notwithstanding, all excitons now carry the same momentum mismatch so it is gauge eliminable, and Eq. (3) realizes the usual Bose-Hubbard Hamiltonian.

We model the light-matter interaction by

$$\hat{V}_{\mathrm{LMI}} = \sum_{\mathbf{p}_\parallel, p_\perp, \sigma} \hbar\omega_{\mathbf{p}} \hat{a}^\dagger_{\mathbf{p}\sigma} \hat{a}_{\mathbf{p}\sigma} + (g_{\mathbf{p}\sigma} \hat{a}^\dagger_{\mathbf{p}\sigma} \hat{\chi}_{\mathbf{K}+\mathbf{p}_\parallel} + \mathrm{H.c.}), \tag{4}$$

where $\hat{a}^\dagger_{\mathbf{p}\sigma}$ creates a photon with momentum $\mathbf{p}$ with the indicated in- and out-of-plane components and polarization σ. We have incorporated the exciton momentum mismatch, and made the rotating-wave approximation [67]. The coupling constants $g_{\mathbf{p}\sigma}$ are obtained from electronic interband transition dipole matrix elements, and depend on the exciton pairing wave function [38] etc. The recombination rate $\Gamma_{\mathbf{k}}$ of each exciton at $\mathbf{k}$ inside the light cone can be computed [38] using Fermi's golden rule [68]. This defines a natural timescale,

the lifetime of a localized exciton in a single moiré site, $\tau_{\rm loc}^{-1} = \frac{1}{N}\sum_{\mathbf{k}\in \rm LC}\Gamma_{\mathbf{k}}$. The relative size of the light cone compared to the total MBZ $= \frac{1}{N}\sum_{\mathbf{k}\in \rm LC} \sim (E_0 a/\hbar c)^2$ gives the fraction of the localized wave function that is contained in the light cone, and provides the estimate $\tau_{\rm loc} \sim (\hbar c/E_0 a)^2/\Gamma_{\mathbf{K}} \sim$ 10 ns [17]. Note $\tau_{\rm loc}$ is not the exciton mean radiative lifetime, which is associated with a thermal averaging over $\Gamma_{\mathbf{k}}$ [38].

Let us assume that exciton recombination is sufficiently slow to maintain quasiequilibrium, with an associated chemical potential μ and grand-canonical potential $\hat{\Xi} = \hat{H} - \mu\hat{N}$. We will study the ground state of the excitonic sector of $\hat{\Xi}$ and treat $\hat{V}_{\rm LMI}$ as a weak perturbation that generates photons which probe it. This picture is made consistent by shifting the photon energies to $(\hbar\omega_{\mathbf{p}} - \mu)$ [50].

Weak interactions: Bogoliubov theory. Though the excitons we consider are strongly interacting [17,49], we first present our emission mechanism in the familiar weakly interacting Bogoliubov theory to build our intuition.

A BEC with all excitons at $\mathbf{k} = \mathbf{0}$ will be depleted by interactions that eject pairs of counterpropagating excitons from the condensate. If one lands within the light cone, it may recombine. Bogoliubov theory lets us neatly resum these virtual processes and find the depleted ground state.

Consider a state with total filling (number of excitons per site) ν and condensate filling $\nu_c(\nu)$. Equation (3) leads to the standard [69] mean-field (MF) Bogoliubov–de Gennes (BdG) Hamiltonian $\hat{\Xi}_{\rm MF} = \sum_{\mathbf{k}} \Omega_{\mathbf{k}} \hat{b}^\dagger_{\mathbf{k}} \hat{b}_{\mathbf{k}}$ with the familiar dispersion $\Omega^2_{\mathbf{k}} = \epsilon_{\mathbf{k}}(\epsilon_{\mathbf{k}} + 2\nu_c U)$, $\mu = E_0 + \nu_c U$, and the Bogoliubov modes

$$\hat{b}_{\mathbf{k}} = \cosh(\theta_{\mathbf{k}})\hat{\chi}_{\mathbf{k}} + \sinh(\theta_{\mathbf{k}})\hat{\chi}^\dagger_{-\mathbf{k}}, \quad \sinh\theta_{\mathbf{k}} = \frac{\Omega_{\mathbf{k}} - \epsilon_{\mathbf{k}}}{2\sqrt{\Omega_{\mathbf{k}}\epsilon_{\mathbf{k}}}}. \quad (5)$$

The ground state of the theory is the BdG vacuum. Yet the mixing of particle creation and annihilation in Eq. (5) implies that it nevertheless contains some excitons also at $\mathbf{k} \neq \mathbf{0}$, most notably inside the light cone.

Consider recombination in terms of the collective modes. Transcribed into BdG modes, Eq. (4) contains terms such as $-g_{\mathbf{p}\sigma}\sinh(\theta_{\mathbf{K}+\mathbf{p}_\parallel})\hat{a}^\dagger_{\mathbf{p}\sigma}\hat{b}^\dagger_{-\mathbf{K}-\mathbf{p}_\parallel}$, which represent a spontaneous emission of a photon and a BdG mode, the latter assuring momentum conservation in analogy to phonon-assisted exciton recombination [5]. Therefore, interactions enable an otherwise-dark exciton condensate to "leak" photons with

$$\hbar\omega_{\mathbf{p}} = \mu - \Omega_{-\mathbf{K}-\mathbf{p}_\parallel} = E_0 + \nu_c U - \Omega_{-\mathbf{K}-\mathbf{p}_\parallel} < E_0. \quad (6)$$

As expected, some energy is lost to the Bogoliubov mode.

We compute the total emission rate Γ with Fermi's golden rule via transitions between the BdG vacuum and single quasiparticle states. The redshift in Eq. (6) is negligible compared to E_0, so this is equivalent to counting the number of excitons present within the light cone,

$$\Gamma \approx \sum_{\mathbf{k}\in \rm LC}\Gamma_{\mathbf{k}} n_{\mathbf{k}} \approx N\tau_{\rm loc}^{-1} n_{\mathbf{K}} \approx N\tau_{\rm loc}^{-1}\left(\frac{1}{18}\frac{\nu_c}{t/U}\right)^2. \quad (7)$$

Here we approximated $n_{\mathbf{k}} = \langle\hat{\chi}^\dagger_{\mathbf{k}}\hat{\chi}_{\mathbf{k}}\rangle \approx n_{\mathbf{K}} = \sinh^2\theta_{\mathbf{K}}$ inside the light cone, assuming it is much smaller than the MBZ, and expanded around small densities. The total filling is found by integrating $n_{\mathbf{k}}$ [69], and in two dimensions $\nu_c = \nu[1 - O(U/t)]$. Thus, unlike spontaneous decay, Γ is quadratic in density.

The generality of this construction suggests that exciton condensates in any indirect-gap system are leaky. Moreover, emission is accomplished without additional degrees of freedom. This contrasts with external optical probing [70] and other mechanisms that involve phonons [71] or carrier exchange in larger exciton complexes [72].

Interactions deplete excitons into excited bands as well, and so leaky condensates can also occur in systems that are dark due to a spin-forbidden transition, etc. Previous studies have shown that, for sufficiently strong interactions (or, equivalently, above a threshold density), a dark condensate can transition into a so-called gray condensate [73–76]. Our finding of leaky emissions is distinct from these previous works: (i) Emission from the leaky condensate grows continuously with increasing density, with no threshold value. (ii) In indirect-gap materials, the bright and (momentum-)dark states are smoothly connected along the same Bloch band, unlike the usual scenario where they are spin-split and form separate bands. This prevents fragmentation into a gray condensate. (iii) The gray condensate emission is coherent whereas the leaky condensate emission is incoherent, due to its entanglement with the generated collective modes.

Condensate depletion by interactions has recently gained significant experimental attention [77–81]. Relatedly, BdG modes are used to renormalize phonon-assisted photoluminescence line shapes, e.g., in Cu_2O [5,82,83]. However, the role of collective modes in *enabling* recombination of indirect-gap excitons, to the best of our knowledge, has not been pointed out so far. Additionally, these descriptions focus on weakly interacting excitons.

Strong interactions: Hard-core bosons. We now explore how leaky condensates manifest under strong interactions. Consider the $U \to \infty$ limit corresponding to hard-core bosons, which, with the transformation ($S = \frac{1}{2}$ henceforth implied)

$$\hat{S}^-_{\mathbf{R}} = e^{-i\mathbf{K}\cdot\mathbf{R}}\hat{\chi}_{\mathbf{R}}, \quad \hat{S}^+_{\mathbf{R}} = e^{i\mathbf{K}\cdot\mathbf{R}}\hat{\chi}^\dagger_{\mathbf{R}}, \quad \hat{S}^z_{\mathbf{R}} = \hat{\chi}^\dagger_{\mathbf{R}}\hat{\chi}_{\mathbf{R}} - S, \quad (8)$$

map to a spin-$\frac{1}{2}$ XX ferromagnet in a transverse field. The grand-canonical potential becomes

$$\hat{\Xi} = -t\sum_{\langle\mathbf{R},\mathbf{R}'\rangle}(\hat{S}^+_{\mathbf{R}'}\hat{S}^-_{\mathbf{R}} + \hat{S}^+_{\mathbf{R}}\hat{S}^-_{\mathbf{R}'}) + (E_0 - \mu)\sum_{\mathbf{R}}\left(\hat{S}^z_{\mathbf{R}} + S\right). \quad (9)$$

The recombination rate remains $\Gamma\tau_{\rm loc}/N \approx n_{\mathbf{K}} = \langle\hat{S}^+_{\mathbf{K}}\hat{S}^-_{\mathbf{K}}\rangle$, where $\hat{S}^-_{\mathbf{K}} = \frac{1}{\sqrt{N}}\sum_{\mathbf{R}} e^{-i\mathbf{K}\cdot\mathbf{R}}\hat{S}^-_{\mathbf{R}}$.

This limit readily manifests ground state emission: With $t = 0$, Eq. (9) factorizes into independent sites each with MF solution $\sqrt{\nu}\,|\Uparrow\rangle + \sqrt{1-\nu}\,|\Downarrow\rangle$, yielding [50] $n_{\mathbf{K}}(\nu) = \nu^2$. As nonzero hopping allows repelling excitons to separate, leading to *anti*correlations, this is an upper bound. Additionally, an emergent particle-vacancy duality [50] $\hat{S}^\pm_{\mathbf{R}} \to \hat{S}^\mp_{\mathbf{R}}$ connects the ground states of Eq. (9) with fillings ν and $1-\nu$, providing the identity $n_{\mathbf{K}}(\nu) - n_{\mathbf{K}}(1-\nu) = 2\nu - 1$. Thus, $n_{\mathbf{K}}(\nu) > \max(2\nu - 1, 0)$. These bounds already demonstrate the interaction-driven nonlinearity of $\Gamma(\nu)$.

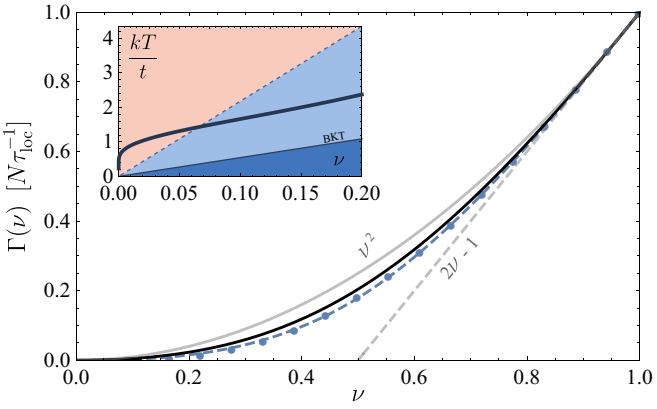

FIG. 2. Emission rate $\Gamma(\nu)$ at $T = 0$ versus filling [86] within the Holstein-Primakoff expansion [50] (solid black), compared with exact diagonalization on a 6×3 lattice (filled circles) and a least-squares fit derived from two-body states (dashed blue). The solid and dashed gray lines are upper and lower bounds explained in the text. Inset: The crossover temperature $T^\star$ between interaction- and thermally-dominated emission. The solid and dashed thin lines mark the Berezinskii-Kosterlitz-Thouless superfluid transition and quantum degeneracy crossover, estimated at $kT/t = \sqrt{3}\pi\nu$ and $4\sqrt{3}\pi\nu$, respectively [50]. Interactions dominate the cold regimes.

A quantitative treatment of emission is again found in terms of spontaneously excited collective modes, now taking the form of spin waves. We perform a Holstein-Primakoff (HP) $1/S$ expansion [84] similar to that of Bernardet *et al.* [85], with details provided in the Supplemental Material [50]. The qualitative features of Bogoliubov theory are reproduced: we obtain a quadratic $\hat{\Xi} = \sum \Omega_{\mathbf{k}} \hat{b}_{\mathbf{k}}^\dagger \hat{b}_{\mathbf{k}}$, now with dispersion $\Omega_{\mathbf{k}}^2 = \epsilon_{\mathbf{k}}[(2\nu_{\rm MF} - 1)^2\epsilon_{\mathbf{k}} + 24\nu_{\rm MF}(1 - \nu_{\rm MF})t]$ and $\mu = E_0 + 6(2\nu_{\rm MF} - 1)$, where the filling $\nu_{\rm MF}$ is the mean-field order parameter (cf. ν_c in the previous section). The exciton occupation in the spin-wave vacuum, or equivalently at temperature $T = 0$, is now

$$n_{\mathbf{k}} = [\nu_{\rm MF} \cosh\theta_{\mathbf{k}} + (1 - \nu_{\rm MF}) \sinh\theta_{\mathbf{k}}]^2. \tag{10}$$

$\theta_{\mathbf{k}}$ and the emission spectra are still given by Eqs. (5) and (6).

We plot the $T = 0$ emission rate $\Gamma \propto n_{\mathbf{K}}$ in Fig. 2 [86]. Comparing it against small-scale exact diagonalization, we find very good agreement across a wide range of fillings. In the dilute limit,

$$\Gamma(\nu \ll 1) \approx \frac{4}{9} N \tau_{\rm loc}^{-1} \nu_{\rm MF}^2. \tag{11}$$

The apparent quadratic dependence in Eq. (11) does not imply an absence of correlations, which cause $\nu_{\rm MF}(\nu)$ and ν to differ. Exciton correlations can be inferred from two-body states [76], from which we deduce [50] the asymptotic form $\Gamma \sim (\nu/\log\nu)^2$, revealing the expected suppression. Numerics confirm [50] that $\nu_{\rm MF} \sim (\nu/\log\nu)$ for $\nu \ll 1$, indicating correlations are successfully captured.

Our HP theory also allows us to treat nonzero temperatures. Thermal excitations enhance emission and unlock a second channel whereby a collective mode is absorbed instead of emitted, leading to two emission lines. In the inset of Fig. 2 we plot the crossover temperature $T^\star$ at which depletion (due to interactions) and thermal excitations contribute equally [50] to the total emission rate, and below which interactions dominate. This crossover occurs above the Berezinskii-Kosterlitz-Thouless (BKT) transition [87,88], indicating that leaky emission will be the dominant emission channel characterizing the superfluid phase and much of the quantum-degenerate regime. Remarkably, in this strongly interacting system, at small filling "leaks" dominate emission even in the hot gas phase that can be treated semiclassically. Unlike the Stokes and anti-Stokes lines in phonon-assisted emission [5], the two BdG processes have unequal matrix elements with different density dependences. The anti-Stokes-like line dominates above $T^\star$, and the net annihilation of BdG modes may evaporatively cool the BEC, similarly to a mechanism recently suggested [89]. Finally, the strength of interactions can be inferred from the ratio of emission line intensities [50].

The leaky condensate picture thus predicts a distinctive property of moiré exciton emission: a dominant redshifted emission line with quadratic density dependence below $T^\star$, compared to a dominant blueshifted line with linear density dependence above $T^\star$. We do not expect a qualitative change at the BKT transition.

Experimental consequences. We assess the parameters under which a leaky condensate may be observed. Comparing Eq. (7) with (11) suggests that this mechanism saturates once $U > 12t$, which should hold across a wide range of twist angles [17]. For $a \approx 10$ nm (twist $\approx 2^\circ$) and corresponding $t \approx 0.2$ meV [17], and at a demonstrated [90] photoexcited exciton density of $n \approx 10^{11}$ cm^{-2} ($\nu \approx 0.1$), $T^\star \approx 5$ K. Larger twist angles or intercalated hBN spacers would increase t and thus $T^\star$ [17,49], and mitigate inhomogeneity effects. Furthermore, electrostatic gating might modify the moiré symmetry [17] or its elastic reconstruction [91,92], allowing *in situ* tunability. Above $T^\star$ the two emission lines are split by $\sim 20t \sim 4$ meV and should be resolvable.

Leaky emission will manifest in a quadratic loss $\partial_t n = -\gamma n^2$, with n the exciton number density. With Eq. (11) and $\tau_{\rm loc} \sim 10$ ns at $a \sim 10$ nm [17] we estimate a rate constant $\gamma \sim a^2/\tau_{\rm loc} \approx 10^{-4}$ cm^2/s. Exciton density is controlled with pumping fluence, and tracked with transient absorption [93,94], emission blueshift [cf. Eq. (6)] [70,74,90], or time-resolved photoluminescence (PL) [90]. These reveal such quadratic dependence, which is attributed to Auger recombination. In TMDs this process is associated with a high-energy conduction band that supports bound excitons at energies close to $2E_0$, making Auger recombination nearly resonant [95,96]. Yet crucially, for nonzero detuning Auger recombination freezes out at $T \to 0$ [97] and leaky emission will dominate. Comparisons at nonzero temperature are not straightforward; estimates are available mostly for room-temperature monolayers, suggesting an intrinsic Auger constant $\gamma \sim 10^{-3}$ cm^2/s [95,98,99]. However, moving to cryogenic temperatures or to bilayers could each reduce γ by orders of magnitude [97,100]. Thus, the dominance of leaky recombination over Auger could feasibly extend to $T^\star$ and above. This unique regime of emission linear in continuous fluence yet nonlinear in *instantaneous* density might be important in interpreting PL experiments. In settings demonstrating population lifetimes

approaching microseconds [9–12], the short "leaky lifetime" $\tau_{\text{leaks}} \sim (\gamma n)^{-1} \sim 10\,\text{ns}$ induced at high fluences could also play a significant role in the complex population dynamics.

Conclusions. We have shown that strong interactions challenge the picture of dark condensates in moiré bilayers, where they dominate optical processes. This prompts further material-specific modeling to compare these effects to other recombination and loss mechanisms. Additionally, while here we mostly considered a single-valley model, the physics of two-valley moiré condensates is very rich. As we remark above, excitonic density waves put such condensates on the verge of optical activation which is prevented only by vestigial rotational symmetry [50]. Therefore, direct emission with long-range phase coherence may be achieved in these systems by external fields, strain, layer separation, and pressure, with possible sensing applications. We leave this and other novel intervalley phenomena to future work.

Data sharing is not applicable to this article as no datasets were generated or analyzed during the current study.

We thank M. Atatüre, D. Kara, C. M. Pursar, A. R.-P. Montblanch, T. F. Heinz, O. Karni, E. Barré, A. Camacho-Guardian, and D. Bennett for fruitful discussions. The support of the Cambridge International Trust, of EPSRC Grants No. EP/P009565/1 and No. EP/P034616/1, and of a Simons Investigator Award are gratefully acknowledged.

[1] D. Snoke, Spontaneous Bose coherence of excitons and polaritons, Science **298**, 1368 (2002).
[2] T. Byrnes, N. Y. Kim, and Y. Yamamoto, Excitonpolariton condensates, Nat. Phys. **10**, 803 (2014).
[3] L. V. Butov, A. C. Gossard, and D. S. Chemla, Macroscopically ordered state in an exciton system, Nature (London) **418**, 751 (2002).
[4] A. A. High, J. R. Leonard, A. T. Hammack, M. M. Fogler, L. V. Butov, A. V. Kavokin, K. L. Campman, and A. C. Gossard, Spontaneous coherence in a cold exciton gas, Nature (London) **483**, 584 (2012).
[5] S. A. Moskalenko and D. W. Snoke, *Bose-Einstein Condensation of Excitons and Biexcitons* (Cambridge University Press, Cambridge, 2000)
[6] K. Tran, J. Choi, and A. Singh, Moiré and beyond in transition metal dichalcogenide twisted bilayers, 2D Mater. **8**, 022002 (2021).
[7] P. Rivera, J. R. Schaibley, A. M. Jones, J. S. Ross, S. Wu, G. Aivazian, P. Klement, K. Seyler, G. Clark, N. J. Ghimire, J. Yan, D. G. Mandrus, W. Yao, and X. Xu, Observation of long-lived interlayer excitons in monolayer $MoSe_2$–WSe_2 heterostructures, Nat. Commun. **6**, 6242 (2015).
[8] M. Palummo, M. Bernardi, and J. C. Grossman, Exciton radiative lifetimes in two-dimensional transition metal dichalcogenides, Nano Lett. **15**, 2794 (2015).
[9] B. Miller, A. Steinhoff, B. Pano, J. Klein, F. Jahnke, A. Holleitner, and U. Wurstbauer, Long-lived direct and indirect interlayer excitons in van der Waals heterostructures, Nano Lett. **17**, 5229 (2017).
[10] P. Nagler, G. Plechinger, M. V. Ballottin, A. Mitioglu, S. Meier, N. Paradiso, C. Strunk, A. Chernikov, P. C. M. Christianen, C. Schüller, and T. Korn, Interlayer exciton dynamics in a dichalcogenide monolayer heterostructure, 2D Mater. **4**, 025112 (2017).
[11] C. Jiang, W. Xu, A. Rasmita, Z. Huang, K. Li, Q. Xiong, and W. B. Gao, Microsecond dark-exciton valley polarization memory in two-dimensional heterostructures, Nat. Commun. **9**, 753 (2018).
[12] A. R.-P. Montblanch, D. M. Kara, I. Paradisanos, C. M. Purser, M. S. G. Feuer, E. M. Alexeev, L. Stefan, Y. Qin, M. Blei, G. Wang, A. R. Cadore, P. Latawiec, M. Lončar, S. Tongay, A. C. Ferrari, and M. Atatüre, Confinement of long-lived interlayer excitons in WS_2/WSe_2 heterostructures, Commun. Phys. **4**, 119 (2021).
[13] C. Jin, E. C. Regan, D. Wang, M. Iqbal Bakti Utama, C. S. Yang, J. Cain, Y. Qin, Y. Shen, Z. Zheng, K. Watanabe, T. Taniguchi, S. Tongay, A. Zettl, and F. Wang, Identification of spin, valley and moiré quasi-angular momentum of interlayer excitons, Nat. Phys. **15**, 1140 (2019).
[14] E. Y. Andrei, D. K. Efetov, P. Jarillo-Herrero, A. H. MacDonald, K. F. Mak, T. Senthil, E. Tutuc, A. Yazdani, and A. F. Young, The marvels of moiré materials, Nat. Rev. Mater. **6**, 201 (2021).
[15] S. Brem, K.-Q. Lin, R. Gillen, J. M. Bauer, J. Maultzsch, J. M. Lupton, and E. Malic, Hybridized intervalley moiré excitons and flat bands in twisted WSe_2 bilayers, Nanoscale **12**, 11088 (2020).
[16] F. Wu, T. Lovorn, and A. H. MacDonald, Topological Exciton Bands in Moiré Heterojunctions, Phys. Rev. Lett. **118**, 147401 (2017).
[17] H. Yu, G.-B. Liu, J. Tang, X. Xu, and W. Yao, Moiré excitons: From programmable quantum emitter arrays to spin-orbit–coupled artificial lattices, Sci. Adv. **3**, e1701696 (2017).
[18] H. Baek, M. Brotons-Gisbert, Z. X. Koong, A. Campbell, M. Rambach, K. Watanabe, T. Taniguchi, and B. D. Gerardot, Highly energy-tunable quantum light from moiré-trapped excitons, Sci. Adv. **6**, eaba8526 (2020).
[19] D. M. Kennes, M. Claassen, L. Xian, A. Georges, A. J. Millis, J. Hone, C. R. Dean, D. N. Basov, A. N. Pasupathy, and A. Rubio, Moiré heterostructures as a condensed-matter quantum simulator, Nat. Phys. **17**, 155 (2021).
[20] M. M. Fogler, L. V. Butov, and K. S. Novoselov, High-temperature superfluidity with indirect excitons in van der Waals heterostructures, Nat. Commun. **5**, 4555 (2014).
[21] O. L. Berman and R. Y. Kezerashvili, High-temperature superfluidity of the two-component Bose gas in a transition metal dichalcogenide bilayer, Phys. Rev. B **93**, 245410 (2016).
[22] D. Jérome, T. M. Rice, and W. Kohn, Excitonic insulator, Phys. Rev. **158**, 462 (1967).
[23] F.-C. Wu, F. Xue, and A. H. MacDonald, Theory of two-dimensional spatially indirect equilibrium exciton condensates, Phys. Rev. B **92**, 165121 (2015).

[24] B. Debnath, Y. Barlas, D. Wickramaratne, M. R. Neupane, and R. K. Lake, Exciton condensate in bilayer transition metal dichalcogenides: Strong coupling regime, Phys. Rev. B **96**, 174504 (2017).

[25] Z. Wang, D. A. Rhodes, K. Watanabe, T. Taniguchi, J. C. Hone, J. Shan, and K. F. Mak, Evidence of high-temperature exciton condensation in two-dimensional atomic double layers, Nature (London) **574**, 76 (2019).

[26] L. Ma, P. X. Nguyen, Z. Wang, Y. Zeng, K. Watanabe, T. Taniguchi, A. H. MacDonald, K. F. Mak, and J. Shan, Strongly correlated excitonic insulator in atomic double layers, Nature (London) **598**, 585 (2021).

[27] J. Gu, L. Ma, S. Liu, K. Watanabe, T. Taniguchi, J. C. Hone, J. Shan, and K. F. Mak, Dipolar excitonic insulator in a moiré lattice, Nat. Phys. **18**, 395 (2022).

[28] Q. Shi, E.-M. Shih, D. Rhodes, B. Kim, K. Barmak, K. Watanabe, T. Taniguchi, Z. Papić, D. A. Abanin, J. Hone, and C. R. Dean, Bilayer WSe_2 as a natural platform for interlayer exciton condensates in the strong coupling limit, Nat. Nanotechnol. (2022), doi: 10.1038/s41565-022-01104-5.

[29] D. N. Basov, M. M. Fogler, and F. J. García de Abajo, Polaritons in van der Waals materials, Science **354**, aag1992 (2016).

[30] M. Förg, L. Colombier, R. K. Patel, J. Lindlau, A. D. Mohite, H. Yamaguchi, M. M. Glazov, D. Hunger, and A. Högele, Cavity-control of interlayer excitons in van der Waals heterostructures, Nat. Commun. **10**, 3697 (2019).

[31] H. Yu and W. Yao, Electrically tunable topological transport of moiré polaritons, Sci. Bull. **65**, 1555 (2020).

[32] L. Zhang, F. Wu, S. Hou, Z. Zhang, Y. H. Chou, K. Watanabe, T. Taniguchi, S. R. Forrest, and H. Deng, Van der Waals heterostructure polaritons with moiré-induced nonlinearity, Nature (London) **591**, 61 (2021).

[33] A. Camacho-Guardian and N. R. Cooper, Moiré-induced optical non-linearities: Single and multi-photon resonances, arXiv:2108.06177.

[34] P. Rivera, H. Yu, K. L. Seyler, N. P. Wilson, W. Yao, and X. Xu, Interlayer valley excitons in heterobilayers of transition metal dichalcogenides, Nat. Nanotechnol. **13**, 1004 (2018).

[35] N. R. Wilson, P. V. Nguyen, K. Seyler, P. Rivera, A. J. Marsden, Z. P. Laker, G. C. Constantinescu, V. Kandyba, A. Barinov, N. D. Hine, X. Xu, and D. H. Cobden, Determination of band offsets, hybridization, and exciton binding in 2D semiconductor heterostructures, Sci. Adv. **3**, e1601832 (2017).

[36] H. Yu, Y. Wang, Q. Tong, X. Xu, and W. Yao, Anomalous Light Cones and Valley Optical Selection Rules of Interlayer Excitons in Twisted Heterobilayers, Phys. Rev. Lett. **115**, 187002 (2015).

[37] In some bilayers, the band gap is indirect at zero twist. However, our theory may still apply over relevant timescales [50].

[38] J. Choi, M. Florian, A. Steinhoff, D. Erben, K. Tran, D. S. Kim, L. Sun, J. Quan, R. Claassen, S. Majumder, J. A. Hollingsworth, T. Taniguchi, K. Watanabe, K. Ueno, A. Singh, G. Moody, F. Jahnke, and X. Li, Twist Angle-Dependent Interlayer Exciton Lifetimes in van der Waals Heterostructures, Phys. Rev. Lett. **126**, 047401 (2021).

[39] C. Zhang, C.-P. Chuu, X. Ren, M.-Y. Li, L.-J. Li, C. Jin, M.-Y. Chou, and C.-K. Shih, Interlayer couplings, Moiré patterns, and 2D electronic superlattices in MoS_2/WSe_2 hetero-bilayers, Sci. Adv. **3**, e1601459 (2017).

[40] F. Wu, T. Lovorn, and A. H. MacDonald, Theory of optical absorption by interlayer excitons in transition metal dichalcogenide heterobilayers, Phys. Rev. B **97**, 035306 (2018).

[41] S. Shabani, D. Halbertal, W. Wu, M. Chen, S. Liu, J. Hone, W. Yao, D. N. Basov, X. Zhu, and A. N. Pasupathy, Deep moiré potentials in twisted transition metal dichalcogenide bilayers, Nat. Phys. **17**, 720 (2021).

[42] H. Guo, X. Zhang, and G. Lu, Shedding light on moiré excitons: A first-principles perspective, Sci. Adv. **6**, eabc5638 (2020).

[43] S. Brem, C. Linderälv, P. Erhart, and E. Malic, Tunable phases of moiré excitons in van der Waals heterostructures, Nano Lett. **20**, 8534 (2020).

[44] K. Tran, G. Moody, F. Wu, X. Lu, J. Choi, K. Kim, A. Rai, D. A. Sanchez, J. Quan, A. Singh, J. Embley, A. Zepeda, M. Campbell, T. Autry, T. Taniguchi, K. Watanabe, N. Lu, S. K. Banerjee, K. L. Silverman, S. Kim *et al.*, Evidence for moiré excitons in van der Waals heterostructures, Nature (London) **567**, 71 (2019).

[45] F. Mahdikhanysarvejahany, D. N. Shanks, C. Muccianti, B. H. Badada, I. Idi, A. Alfrey, S. Raglow, M. R. Koehler, D. G. Mandrus, T. Taniguchi, K. Watanabe, O. L. A. Monti, H. Yu, B. J. LeRoy, and J. R. Schaibley, Temperature dependent moiré trapping of interlayer excitons in $MoSe_2 - WSe_2$ heterostructures, npj 2D Mater Appl **5**, 67 (2021).

[46] O. Karni, E. Barré, V. Pareek, J. D. Georgaras, M. K. L. Man, C. Sahoo, D. R. Bacon, X. Zhu, H. B. Ribeiro, A. L. O'Beirne, J. Hu, A. Al-Mahboob, M. M. M. Abdelrasoul, N. S. Chan, A. Karmakar, A. J. Winchester, B. Kim, K. Watanabe, T. Taniguchi, K. Barmak *et al.*, Structure of the moiré exciton captured by imaging its electron and hole, Nature (London) **603**, 247 (2022).

[47] C. Jin, E. C. Regan, A. Yan, M. Iqbal Bakti Utama, D. Wang, S. Zhao, Y. Qin, S. Yang, Z. Zheng, S. Shi, K. Watanabe, T. Taniguchi, S. Tongay, A. Zettl, and F. Wang, Observation of moiré excitons in WSe_2/WS_2 heterostructure superlattices, Nature (London) **567**, 76 (2019).

[48] K. L. Seyler, P. Rivera, H. Yu, N. P. Wilson, E. L. Ray, D. G. Mandrus, J. Yan, W. Yao, and X. Xu, Signatures of moiré-trapped valley excitons in $MoSe_2/WSe_2$ heterobilayers, Nature (London) **567**, 66 (2019).

[49] C. Lagoin and F. Dubin, Key role of the moiré potential for the quasicondensation of interlayer excitons in van der Waals heterostructures, Phys. Rev. B **103**, L041406 (2021).

[50] See Supplemental Material at http://link.aps.org/supplemental/10.1103/PhysRevResearch.4.L022042 for additional details on the moiré geometry, symmetry-breaking exciton density waves, and the hard-core spin-wave expansion, including emission spectrum, temperature dependence, density scaling and numerical results.

[51] M. P. A. Fisher, P. B. Weichman, G. Grinstein, and D. S. Fisher, Boson localization and the superfluid-insulator transition, Phys. Rev. B **40**, 546 (1989).

[52] P. Rivera, K. L. Seyler, H. Yu, J. R. Schaibley, J. Yan, D. G. Mandrus, W. Yao, and X. Xu, Valley-polarized exciton dynamics in a 2D semiconductor heterostructure, Science **351**, 688 (2016).

[53] Y. Shimazaki, C. Kuhlenkamp, I. Schwartz, T. Smoleński, K. Watanabe, T. Taniguchi, M. Kroner, R. Schmidt, M. Knap, and

A. Imamoglu, Optical Signatures of Periodic Charge Distribution in a Mott-like Correlated Insulator State, Phys. Rev. X **11**, 021027 (2021).

[54] T. Smoleński, P. E. Dolgirev, C. Kuhlenkamp, A. Popert, Y. Shimazaki, P. Back, X. Lu, M. Kroner, K. Watanabe, T. Taniguchi, I. Esterlis, E. Demler, and A. Imamoglu, Signatures of Wigner crystal of electrons in a monolayer semiconductor, Nature (London) **595**, 53 (2021).

[55] J. Joshi, B. Scharf, I. Mazin, S. Krylyuk, D. J. Campbell, J. Paglione, A. Davydov, I. Žutić, and P. M. Vora, Charge density wave activated excitons in $TiSe_2$-$MoSe_2$ heterostructures, APL Mater. **10**, 011103 (2022).

[56] B. I. Halperin and T. M. Rice, Possible anomalies at a semimetal-semiconductor transition, Rev. Mod. Phys. **40**, 755 (1968).

[57] A. Kogar, M. S. Rak, S. Vig, A. A. Husain, F. Flicker, Y. I. Joe, L. Venema, G. J. MacDougall, T. C. Chiang, E. Fradkin, J. Van Wezel, and P. Abbamonte, Signatures of exciton condensation in a transition metal dichalcogenide, Science **358**, 1314 (2017).

[58] R. Ozeri, N. Katz, J. Steinhauer, and N. Davidson, Colloquium: Bulk Bogoliubov excitations in a Bose-Einstein condensate, Rev. Mod. Phys. **77**, 187 (2005).

[59] S. Utsunomiya, L. Tian, G. Roumpos, C. W. Lai, N. Kumada, T. Fujisawa, M. Kuwata-Gonokami, A. Löffler, S. Höfling, A. Forchel, and Y. Yamamoto, Observation of Bogoliubov excitations in exciton-polariton condensates, Nat. Phys. **4**, 700 (2008).

[60] D. Werdehausen, T. Takayama, M. Höppner, G. Albrecht, A. W. Rost, Y. Lu, D. Manske, H. Takagi, and S. Kaiser, Coherent order parameter oscillations in the ground state of the excitonic insulator Ta_2NiSe_5, Sci. Adv. **4**, eaap8652 (2018).

[61] B. Remez and N. R. Cooper, Effects of disorder on the transport of collective modes in an excitonic condensate, Phys. Rev. B **101**, 235129 (2020).

[62] D. Golež, Z. Sun, Y. Murakami, A. Georges, and A. J. Millis, Nonlinear Spectroscopy of Collective Modes in an Excitonic Insulator, Phys. Rev. Lett. **125**, 257601 (2020).

[63] E. Estrecho, M. Pieczarka, M. Wurdack, M. Steger, K. West, L. N. Pfeiffer, D. W. Snoke, A. G. Truscott, and E. A. Ostrovskaya, Low-Energy Collective Oscillations and Bogoliubov Sound in an Exciton-Polariton Condensate, Phys. Rev. Lett. **126**, 075301 (2021).

[64] H. M. Bretscher, P. Andrich, Y. Murakami, D. Golež, B. Remez, P. Telang, A. Singh, L. Harnagea, N. R. Cooper, A. J. Millis, P. Werner, A. K. Sood, and A. Rao, Imaging the coherent propagation of collective modes in the excitonic insulator Ta_2NiSe_5 at room temperature, Sci. Adv. **7**, eabd6147 (2021).

[65] L. Zhang, R. Gogna, G. W. Burg, J. Horng, E. Paik, Y.-H. Chou, K. Kim, E. Tutuc, and H. Deng, Highly valley-polarized singlet and triplet interlayer excitons in van der Waals heterostructure, Phys. Rev. B **100**, 041402(R) (2019).

[66] G. Scuri, T. I. Andersen, Y. Zhou, D. S. Wild, J. Sung, R. J. Gelly, D. Bérubé, H. Heo, L. Shao, A. Y. Joe, A. M. Mier Valdivia, T. Taniguchi, K. Watanabe, M. Lončar, P. Kim, M. D. Lukin, and H. Park, Electrically Tunable Valley Dynamics in Twisted WSe_2/WSe_2 Bilayers, Phys. Rev. Lett. **124**, 217403 (2020).

[67] M. O. Scully and M. S. Zubairy, *Quantum Optics* (Cambridge University Press, Cambridge, 1997).

[68] J. J. Sakurai and J. Napolitano, *Modern Quantum Mechanics*, 2nd ed. (Cambridge University Press, Cambridge, 2017).

[69] L. Pitaevskii and S. Stringari, *Bose-Einstein Condensation and Superfluidity* (Oxford University Press, Oxford, 2016).

[70] M. Combescot, R. Combescot, M. Alloing, and F. Dubin, Optical signatures of a fully dark exciton condensate, Europhys. Lett. **105**, 47011 (2014).

[71] M. Danovich, V. Zólyomi, V. I. Fal'ko, and I. L. Aleiner, Auger recombination of dark excitons in WS_2 and WSe_2 monolayers, 2D Mater. **3**, 035011 (2016).

[72] M. Danovich, V. Zólyomi, and V. I. Fal'ko, Dark trions and biexcitons in WS_2 and WSe_2 made bright by e-e scattering, Sci. Rep. **7**, 45998 (2017).

[73] R. Combescot and M. Combescot, "Gray" BCS Condensate of Excitons and Internal Josephson Effect, Phys. Rev. Lett. **109**, 026401 (2012).

[74] M. Alloing, M. Beian, M. Lewenstein, D. Fuster, Y. González, L. González, R. Combescot, M. Combescot, and F. Dubin, Evidence for a Bose-Einstein condensate of excitons, Europhys. Lett. **107**, 10012 (2014).

[75] M. Combescot, R. Combescot, and F. Dubin, Bose–Einstein condensation and indirect excitons: a review, Rep. Prog. Phys. **80**, 066501 (2017).

[76] Y. Mazuz-Harpaz, K. Cohen, M. Leveson, K. West, L. Pfeiffer, M. Khodas, and R. Rapaport, Dynamical formation of a strongly correlated dark condensate of dipolar excitons, Proc. Natl. Acad. Sci. USA **116**, 18328 (2019).

[77] K. Xu, Y. Liu, D. E. Miller, J. K. Chin, W. Setiawan, and W. Ketterle, Observation of Strong Quantum Depletion in a Gaseous Bose-Einstein Condensate, Phys. Rev. Lett. **96**, 180405 (2006).

[78] R. Chang, Q. Bouton, H. Cayla, C. Qu, A. Aspect, C. I. Westbrook, and D. Clément, Momentum-Resolved Observation of Thermal and Quantum Depletion in a Bose Gas, Phys. Rev. Lett. **117**, 235303 (2016).

[79] R. Lopes, C. Eigen, N. Navon, D. Clément, R. P. Smith, and Z. Hadzibabic, Quantum Depletion of a Homogeneous Bose-Einstein Condensate, Phys. Rev. Lett. **119**, 190404 (2017).

[80] M. Pieczarka, E. Estrecho, M. Boozarjmehr, O. Bleu, M. Steger, K. West, L. N. Pfeiffer, D. W. Snoke, J. Levinsen, M. M. Parish, A. G. Truscott, and E. A. Ostrovskaya, Observation of quantum depletion in a non-equilibrium exciton-polariton condensate, Nat. Commun. **11**, 429 (2020).

[81] M. Steger, R. Hanai, A. O. Edelman, P. B. Littlewood, D. W. Snoke, J. Beaumariage, B. Fluegel, K. West, L. N. Pfeiffer, and A. Mascarenhas, Direct observation of the quantum fluctuation driven amplitude mode in a microcavity polariton condensate, Phys. Rev. B **103**, 205125 (2021).

[82] H. Haug and H. H. Kranz, Bose-Einstein condensation in nonequilibrium systems, Z. Phys. B **53**, 151 (1983).

[83] H. Shi, G. Verechaka, and A. Griffin, Theory of the decay luminescence spectrum of a Bose-condensed interacting exciton gas, Phys. Rev. B **50**, 1119 (1994).

[84] T. Holstein and H. Primakoff, Field Dependence of the Intrinsic Domain Magnetization of a Ferromagnet, Phys. Rev. **58**, 1098 (1940).

[85] K. Bernardet, G. G. Batrouni, J.-L. Meunier, G. Schmid, M. Troyer, and A. Dorneich, Analytical and numerical study of hardcore Bosons in two dimensions, Phys. Rev. B **65**, 104519 (2002).

[86] The Holstein-Primakoff approximation is generally nonconserving. To recover the particle-vacancy duality of Eq. (9), in Fig. 2 we plot $\Gamma(\nu)$ versus ν_{MF} [50].

[87] V. L. Berezinskii, Destruction of long-range order in one-dimensional and two-dimensional systems possessing a continuous symmetry group. II. Quantum systems, Zh. Eksp. Teor. Fiz. **61**, 1144 (1971) [Sov. Phys. JETP **34**, 610 (1972)].

[88] J. M. Kosterlitz and D. J. Thouless, Ordering, metastability and phase transitions in two-dimensional systems, J. Phys. C: Solid State Phys. **6**, 1181 (1973).

[89] S. Misra, M. Stern, V. Umansky, and I. B. Joseph, Formation dynamics and evaporative cooling of a dark exciton condensate, arXiv:2109.04072.

[90] Z. Wang, Y.-H. Chiu, K. Honz, K. F. Mak, and J. Shan, Electrical tuning of interlayer exciton gases in WSe_2 bilayers, Nano Lett. **18**, 137 (2018).

[91] T. I. Andersen, G. Scuri, A. Sushko, K. De Greve, J. Sung, Y. Zhou, D. S. Wild, R. J. Gelly, H. Heo, D. Bérubé, A. Y. Joe, L. A. Jauregui, K. Watanabe, T. Taniguchi, P. Kim, H. Park, and M. D. Lukin, Excitons in a reconstructed moiré potential in twisted WSe_2/WSe_2 homobilayers, Nat. Mater. **20**, 480 (2021).

[92] D. Bennett and B. Remez, On electrically tunable stacking domains and ferroelectricity in moiré superlattices, npj 2D Mater Appl **6**, 7 (2022).

[93] D. Sun, Y. Rao, G. A. Reider, G. Chen, Y. You, L. Brézin, A. R. Harutyunyan, and T. F. Heinz, Observation of rapid exciton–exciton annihilation in monolayer molybdenum disulfide, Nano Lett. **14**, 5625 (2014).

[94] C. Poellmann, P. Steinleitner, U. Leierseder, P. Nagler, G. Plechinger, M. Porer, R. Bratschitsch, C. Schüller, T. Korn, and R. Huber, Resonant internal quantum transitions and femtosecond radiative decay of excitons in monolayer WSe_2, Nat. Mater. **14**, 889 (2015).

[95] A. Steinhoff, F. Jahnke, and M. Florian, Microscopic theory of exciton-exciton annihilation in two-dimensional semiconductors, Phys. Rev. B **104**, 155416 (2021).

[96] K.-Q. Lin, C. S. Ong, S. Bange, P. E. Faria Junior, B. Peng, J. D. Ziegler, J. Zipfel, C. Bäuml, N. Paradiso, K. Watanabe, T. Taniguchi, C. Strunk, B. Monserrat, J. Fabian, A. Chernikov, D. Y. Qiu, S. G. Louie, and J. M. Lupton, Narrow-band high-lying excitons with negative-mass electrons in monolayer WSe_2, Nat. Commun. **12**, 5500 (2021).

[97] D. Erkensten, S. Brem, K. Wagner, R. Gillen, R. Perea-Causín, J. D. Ziegler, T. Taniguchi, K. Watanabe, J. Maultzsch, A. Chernikov, and E. Malic, Dark exciton-exciton annihilation in monolayer WSe_2, Phys. Rev. B **104**, L241406 (2021).

[98] Y. Hoshi, T. Kuroda, M. Okada, R. Moriya, S. Masubuchi, K. Watanabe, T. Taniguchi, R. Kitaura, and T. Machida, Suppression of exciton-exciton annihilation in tungsten disulfide monolayers encapsulated by hexagonal boron nitrides, Phys. Rev. B **95**, 241403(R) (2017).

[99] J. Zipfel, M. Kulig, R. Perea-Causín, S. Brem, J. D. Ziegler, R. Rosati, T. Taniguchi, K. Watanabe, M. M. Glazov, E. Malic, and A. Chernikov, Exciton diffusion in monolayer semiconductors with suppressed disorder, Phys. Rev. B **101**, 115430 (2020).

[100] L. Yuan and L. Huang, Exciton dynamics and annihilation in WS_2 2D semiconductors, Nanoscale **7**, 7402 (2015).